Cold exposure causes cell death by depolarization-mediated Ca^{2+} overload in a chill-susceptible insect

Jeppe Seamus Bayley[a,1], Christian Bak Winther[a], Mads Kuhlmann Andersen[a], Camilla Grønkjær[a], Ole Bækgaard Nielsen[b], Thomas Holm Pedersen[c], and Johannes Overgaard[a]

[a]Zoophysiology, Department of Bioscience, Aarhus University, 8000 Aarhus C, Denmark; [b]Department of Public Health, Aarhus University, 8000 Aarhus C, Denmark; and [c]Department of Biomedicine, Aarhus University, 8000 Aarhus C, Denmark

Edited by David L. Denlinger, The Ohio State University, Columbus, OH, and approved August 29, 2018 (received for review August 7, 2018)

Cold tolerance of insects is arguably among the most important traits defining their geographical distribution. Even so, very little is known regarding the causes of cold injury in this species-rich group. In many insects it has been observed that cold injury coincides with a cellular depolarization caused by hypothermia and hyperkalemia that develop during chronic cold exposure. However, prior studies have been unable to determine if cold injury is caused by direct effects of hypothermia, by toxic effects of hyperkalemia, or by the depolarization that is associated with these perturbations. Here we use a fluorescent DNA-staining method to estimate cell viability of muscle and hindgut tissue from *Locusta migratoria* and show that the cellular injury is independent of the direct effects of hypothermia or toxic effects of hyperkalemia. Instead, we show that chill injury develops due to the associated cellular depolarization. We further hypothesized that the depolarization-induced injury was caused by opening of voltage-sensitive Ca^{2+} channels, causing a Ca^{2+} overload that triggers apoptotic/necrotic pathways. In accordance with this hypothesis, we show that hyperkalemic depolarization causes a marked increase in intracellular Ca^{2+} levels. Furthermore, using pharmacological manipulation of intra- and extracellular Ca^{2+} concentrations as well as Ca^{2+} channel conductance, we demonstrate that injury is prevented if transmembrane Ca^{2+} flux is prevented by removing extracellular Ca^{2+} or blocking Ca^{2+} influx. Together these findings demonstrate a causal relationship between cold-induced hyperkalemia, depolarization, and the development of chill injury through Ca^{2+}-mediated necrosis/apoptosis.

cold injury | insect | hyperkalemia | depolarization | calcium

The ability to endure climatic extremes is arguably among the most important traits determining the fundamental niche of species (1, 2). This is also true for insects, in which species distribution patterns are found to correlate closely with species thermal tolerance and with cold tolerance in particular (3–5). From a physiological perspective, insects respond to stressful cold with one of three strategies. Freeze-avoiding species are able to stabilize their supercooled body fluids by increasing the concentration of cryoprotectans and by removing ice nucleators (6, 7). Such species can survive low temperature exposure as long as the injurious ice crystallization is prevented (7–9). Another strategy is used by freeze-tolerant species that have adapted to survive substantial ice formation in their extracellular fluids (6, 10). However, the amount of extracellular ice formation increases as temperature is lowered, leading to excessive cellular shrinking and concentrations of solutes that are believed to be major causes of injury in freeze-tolerant insects (5, 8). Chill-susceptible insects comprise the third cold-tolerance category. Insects in this group, which represents the great majority of all insect species, die from effects of temperature that are unrelated to ice formation (9, 11, 12). At present, very little is known about the proximal cause of cold mortality in chill-susceptible species.

It is clear that chill-susceptible species develop cold injury from either direct or indirect effects of low temperature that are independent of the ice/water transition (13–15). It is also clear that the development of chill injury increases with the duration and intensity of the cold exposure (14, 16, 17). It has been proposed that the direct cause of cellular chill injury is a cold-induced membrane phase transition that disrupts cellular integrity (18–20). To our knowledge, no studies have directly investigated membrane phase transitions in insects, but this hypothesis is consistent with the observation that chill injury increases with the duration and intensity of cold. An additional hypothesis related to chill injury proposes that injury develops as an indirect consequence of reduced active transport at low temperature. This hypothesis suggests that hypothermia reduces active transport rates more than passive diffusion rates (14, 21, 22) and that these disproportionate effects cause a dissipation of ion balance, leading to chill injury (14–16). The hypothesis of indirect chill injury is supported by correlative observations that insect chill injury consistently coincides with a massive increase in the extracellular K^+ concentration (13, 15, 22, 23). However, despite the overwhelming correlative evidence linking hyperkalemia and chill injury, no studies have directly demonstrated a mechanistic link. Nevertheless, it has been suggested that injury is caused by membrane depolarization induced by the combined effects of hypothermia and hyperkalemia (23–25). A plausible mechanism for this relation was proposed in two classic reviews on hypothermia and hypoxia (26, 27). These reviews suggested that chronic cell depolarization could activate voltage-gated Ca^{2+} channels, causing an uncontrolled cellular influx of Ca^{2+} that initiates apoptotic and/or necrotic pathways. A link between hypothermia and Ca^{2+} influx has previously been documented in

Significance

Insects comprise the largest class of animals and include numerous species of direct importance to humans, including pests and pollinators. Cold tolerance is arguably among the most important traits determining the distribution of insects. Hypothermia has been proposed to induce cell injury directly by promoting membrane phase transitions resulting in cell leak. Additionally, hypothermia induces hemolymph hyperkalemia, and it has been proposed that hypothermia induces injury indirectly through the resulting depolarization by inducing Ca^{2+} influx promoting apoptosis/necrosis. Here we show that depolarization is a principal mechanism for hypothermic cell injury. Furthermore, we show that intracellular Ca^{2+} increases upon depolarization and that this increase must flux through Ca^{2+} channels in the membrane to accumulate and induce injury.

Author contributions: J.S.B., O.B.N., T.H.P., and J.O. designed research; J.S.B., C.B.W., M.K.A., and C.G. performed research; J.S.B., C.B.W., C.G., and J.O. analyzed the data; J.S.B., C.B.W., and J.O. wrote the paper; and J.S.B., C.B.W., M.K.A., O.B.N., T.H.P., and J.O. revised the final version of the paper.

The authors declare no conflict of interest.

This article is a PNAS Direct Submission.

[1]To whom correspondence should be addressed. Email: jeppe.bayley@bios.au.dk.

Published online September 25, 2018.

plants, mammals, and insects (28–34), in which it has been associated with either cell damage (28, 33, 34) or cold resistance (29–32). However, while several authors have proposed that apoptotic mechanisms are involved in insect chill injury (24, 32, 35–37), the hypothesized link between membrane potential (V_m) and cell injury has not been directly documented. Thus, while several findings imply a causal relationship between V_m and the manifestation of chill injury, it remains to be shown that injury onset can be achieved by V_m depolarization independent of changes in temperature and/or extracellular K^+. Furthermore, it is unknown how depolarization could cause injury in insects.

In the present study we examine the hypothesis that cold-induced cell injury develops primarily as a consequence of depolarization using muscle fibers and hindgut tissue from the tropical (i.e., chill-susceptible) migratory locust (*Locusta migratoria*). Furthermore, we hypothesize that the mechanism of depolarization-induced cell injury is caused by uncontrolled influx of Ca^{2+} from the extracellular space, which triggers cell death. The present study provides compelling evidence of a causal relationship between cell depolarization and chill-induced cell injury. In addition, by adding Ca^{2+} chelators or blocking the Ca^{2+} channels, we provide evidence that development of cell injury following depolarization is dependent on Ca^{2+} influx from the extracellular compartment.

Results

Effects of Extracellular K^+ and Temperature on V_m and Cell Viability. The effects of hyperkalemia and hypothermia on muscle V_m were examined by exposing muscle tissue to buffers containing K^+ concentrations of 5, 10, 30, 50, or 120 mM at either 31 °C or 0 °C. As expected, both hypothermia and hyperkalemia caused depolarization of V_m (two-way ANOVA, effect of hypothermia: $F_{1,413} = 88.1$; $P < 0.0001$; effect of hyperkalemia: $F_{1,413} = 413.8$; $P < 0.0001$) (Fig. 1*A*). Cell viability was examined in a parallel set of preparations using the same combinations of temperature and hyperkalemia. In buffers with control K^+ concentrations (10 mM) viability remained high (~90%) at both experimental temperatures, indicating that the dissection protocol was relatively noninvasive (Fig. 1*B*). Increasing extracellular K^+ concentrations reduced viability so that injury started to develop to an increasing degree under conditions in which V_m depolarized further than −30 mV (two-way ANOVA, effect of hypothermia on viability: $F_{1,146} = 12.4$; $P < 0.001$; effect of hyperkalemia on viability: $F_{1.146} = 183.5$; $P < 0.0001$) (Fig. 1*B*). The additive effects of hypothermia and hyperkalemia are also evident from the observation that onset of injury required a higher extracellular K^+ concentration at 31 °C than at 0 °C (viability was significantly lower than in controls at 120 and 30 mM K^+ for warm and cold preparations, respectively). Combining data from warm and cold preparations as a function of V_m revealed a single sigmoidal pattern (Fig. 1*C*). That is, modest depolarization of the cells caused no significant increase in cellular injury, while more extreme depolarization gave rise to substantial injury. From the sigmoidal fit, the V_m resulting in a 50% reduction in viability (V_{m50}) relative to the controls was −14 mV.

An additional set of experiments was conducted on ileum tissue to examine if the relationship between V_m and cellular viability was found in other tissues when subjected to hypothermia or hyperkalemia. In accordance with the results from muscle fibers, both low temperature and high K^+ depolarized ileum cells (two-way ANOVA, effect of hypothermia: $F_{1,25} = 36.44$; $P < 0.0001$; effect of hyperkalemia: $F_{1,25} = 19.93$; $P < 0.0001$) (Fig. 2*A*). Furthermore, as in muscle cells, low temperature and high K^+ both caused cellular injury (two-way ANOVA, effect of hypothermia: $F_{1,85} = 380.41$; $P < 0.0001$; effect of hyperkalemia: $F_{1,85} = 91.19$; $P < 0.0001$) (Fig. 2*B*).

Pharmacological interventions were used in a final set of experiments examining the relationship between cell polarization and cell viability. Muscle fibers were placed in a warm (31 °C) 10-mM K^+ buffer and were depolarized with either 1 or 15 mM tetraethylammonium chloride (TEA), a K^+-channel blocker, to test if injury developed in fibers depolarized in a manner independent of temperature and K^+ concentration. As expected TEA depolarized the fibers in a concentration-dependent manner (one-way ANOVA, effect of TEA on V_m: $F_{1,134} = 123.18$; $P < 0.0001$) (Fig. 3*A*). Furthermore, in accordance with our hypothesis, injury developed in conjunction with the loss of cell potential (one-way ANOVA, effect of TEA on viability: $F_{1,40} = 66.49$; $P < 0.0001$) (Fig. 3*B*). The 1-mM TEA treatment caused a small (5-mV) depolarization that did not significantly reduce fiber viability (~87% viability) below control values (~89% viability), while 15 mM TEA caused both a substantial depolarization (~22 mV depolarized relative to the control) and a substantial loss of fiber viability (dropped to ~48%) (Fig. 3*B*).

The Role of Ca^{2+} for Viability. To investigate if chronic depolarization induces an alteration in intracellular Ca^{2+} concentration, the cellular Ca^{2+} concentration was followed by an injection of Fluo-4 into muscle fibers. The subsequent fluorescence signal was then measured in fibers exposed to control (10-mM K^+) or hyperkalemic buffers (50- or 120-mM K^+). These experiments showed that the fluorescence signal increased transiently in the 120-mM K^+ buffer (two-way ANOVA, effect of K^+: $F_{2,104} = 1.268$; $P = 0.316$; effect of time: $F_{6,104} = 11.054$; $P < 0.001$; interaction: $F_{12,104} = 4.257$; $P < 0.001$). A similar trend was observed in fibers subjected to the 50-mM K^+ buffer but was not statistically significant.

An additional series of experiments was conducted to investigate if cellular injury was induced by a depolarization-induced flux of Ca^{2+} through Ca^{2+} channels. In these experiments we manipulated extracellular or intracellular Ca^{2+} availability as well as sarcolemmal Ca^{2+} flux using pharmacological interventions. These experiments were performed on muscle fibers exposed to 10 mM or 50 mM K^+ at 0 °C for 24 h. The results show a significant effect of both K^+ and the pharmacological interventions (two-way ANOVA, effect of K^+ on viability: $F_{1,125} = 24.9$; $P < 0.0001$; effect of pharmacological intervention: $F_{3,125} = 16.52$; $P < 0.0001$; interaction: $F_{3,125} = 18.51$; $P < 0.0001$). Thus, the control experiments confirmed that hyperkalemia induced a significant reduction in viability (Fig. 4*B*). However, the viability of hyperkalemic fibers was retained when Ca^{2+} was removed from the extracellular medium by adding EGTA, a membrane-impermeable Ca^{2+} chelator. Removal of intracellular Ca^{2+} with 1,2-Bis(2-aminophenoxy)ethane-*N*,*N*,*N*′,*N*′-tetraacetic acid actoxymethyl ester (BAPTA-AM), a membrane-permeable Ca^{2+} chelator, also prevented cellular injury. Finally, blocking Ca^{2+} entry into the intracellular space using lanthanum (III) chloride ($LaCl_3$), a Ca^{2+} channel blocker, also prevented cellular injury (Fig. 4*B*). Note also that none of these pharmacological interventions affected cellular viability when applied in a control (10-mM) buffer.

Discussion

Loss of V_m Initiates Cell Death. Locusts, like many tropical, subtropical, and temperate insects, are considered to be chill sensitive (3, 15). The mechanism for hypothermic injury in chill-sensitive insects has been debated, and it has been suggested that injury could occur directly through membrane phase transitions and/or indirectly through depolarization and loss of ion balance. The present study was designed to examine if chill injury in insects is caused by (*i*) direct effects of low temperature exposure, (*ii*) cellular depolarization, or (*iii*) a toxic effect of hyperkalemia apart from depolarization. Our results demonstrate that cell injury develops in a manner that is dependent on the degree of membrane depolarization. Thus, for muscle fibers, hypothermia and hyperkalemia independently depolarized the

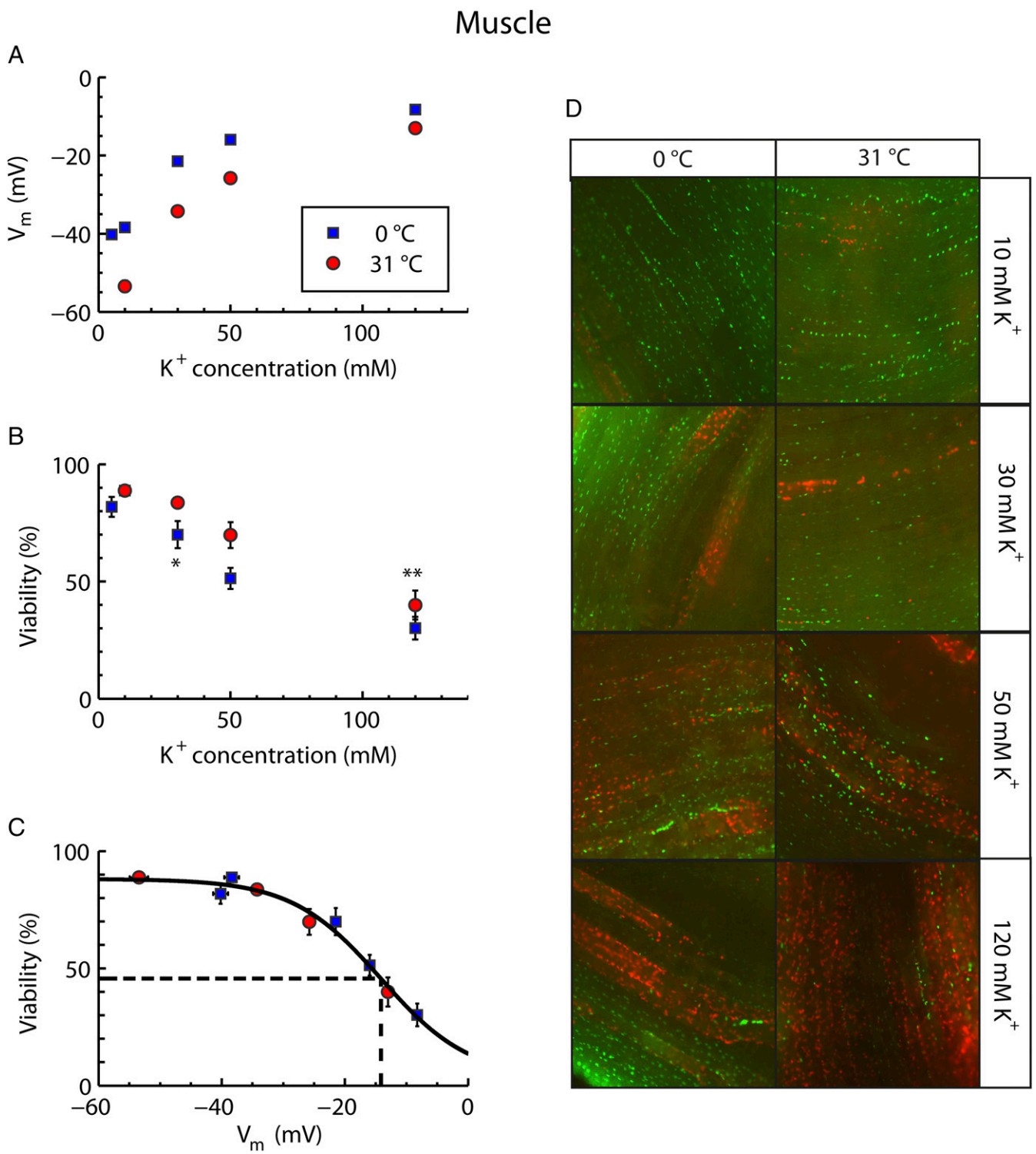

Fig. 1. Relation between V_m and cellular viability in locust muscle exposed to hyperkalemia and hypothermia. Viability measurements were taken after 24 and 3 h, and V_m was measured after 45 and 5 min at 0 °C and 31 °C, respectively (*Materials and Methods*). (*A*) V_m as a function of extracellular K^+ concentration. Note that the error bars are obscured by the symbols. (*B*) Muscle fiber viability as a function of extracellular K^+ concentration. Note that cold fibers at 10 mM K^+ are hidden by the symbol for the warm fibers. (*C*) Muscle fiber viability plotted against V_m. The solid line shows a sigmoidal fit of all data, and the dashed line indicates the estimated value for V_{m50} (−14 mV). All data are expressed as mean ± SEM Single and double asterisks indicate the first hyperkalemic treatment that results in a significant reduction in viability compared with the 10-mM control for the 0 °C and 31 °C treatments, respectively (two-way ANOVA, Tukey's multiple-comparisons test, $P < 0.05$). For average V_m: $n = \geq 40$ fibers from six or more animals for each treatment; for average viabilities: $n = \geq 13$ animals for each treatment. (*D*) Composite images representative of different treatment groups. Living cells were stained green with SYBR 14, and dead cells were stained red with PI. Each image is 750 pixels across which corresponds to roughly 1 mm.

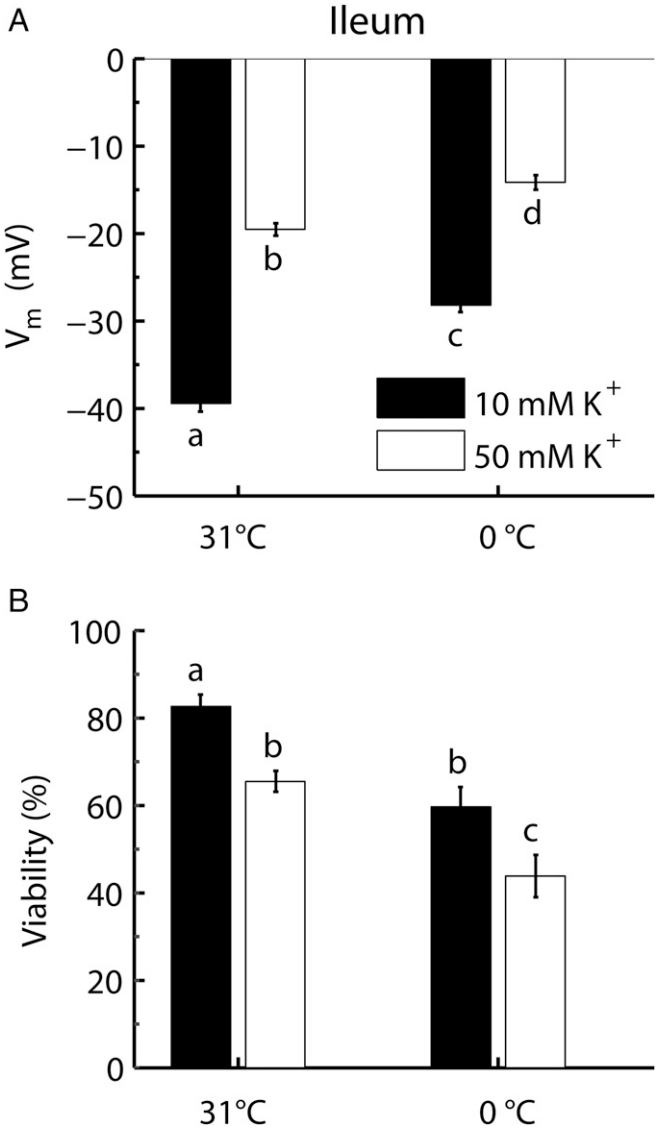

Fig. 2. V_m and cellular viability in ileum cells exposed to hyperkalemia and hypothermia. V_m (*A*) and cell viability (*B*) of ileum cells were measured at 31 °C or 0 °C. The preparations were exposed to 10 or 50 mM K^+. Viability measurements were taken after 24 and 3 h, and V_m was measured after 45 and 5 min at 0 °C and 31 °C, respectively (*Materials and Methods*). Data are expressed as mean ± SEM; dissimilar letters indicate treatment groups that differ significantly (two-way ANOVA, Tukey's multiple-comparisons test, $P < 0.05$). For average V_m: $n = 22$ cells from six animals for each treatment; for average viabilities: $n = 7$ animals for each treatment.

V_m, and chill injury developed to the same degree at both temperatures when they were depolarized to a similar V_m (Fig. 1 *A*–*C*). Cooling causes cellular depolarization, possibly because it reduces the electrogenic contribution of active ion transport to the V_m, while hyperkalemia causes depolarization by reducing the chemical gradient of K^+ across the membrane (15, 25, 38, 39, 40). The effects of temperature and hyperkalemia on V_m are therefore additive, and we observe the onset of injury at a lower K^+ concentration at low temperature compared with high temperature treatments (Fig. 1*B*). The additive effects of hyperkalemia and low temperature on injury have been shown previously (24), but here we show that injury can also develop at high temperature if the cells are depolarized sufficiently by increasing the K^+ concentration (Fig. 1 *A* and *B*). To exclude the possibility that the association between membrane depolarization and injury is a muscle-specific phenomenon, we also investigated this relation in hindgut tissue (ileum). Again, we found that hypothermia and hyperkalemia had additive effects on V_m in ileum and that injury develops in parallel with the degree of depolarization (Fig. 2). This supports the notion that the detrimental effects of chronic depolarization occur in many tissues when insects are exposed to stressful cold and cold-induced hyperkalemia. Finally, to exclude the possibility that injury is caused by effects of hyperkalemia independent of depolarization (toxic effects) and low temperature (direct temperature effects), we investigated if injury would develop when the V_m was pharmacologically manipulated using TEA, a K^+ channel blocker that causes cellular depolarization. In accordance with our hypothesis,

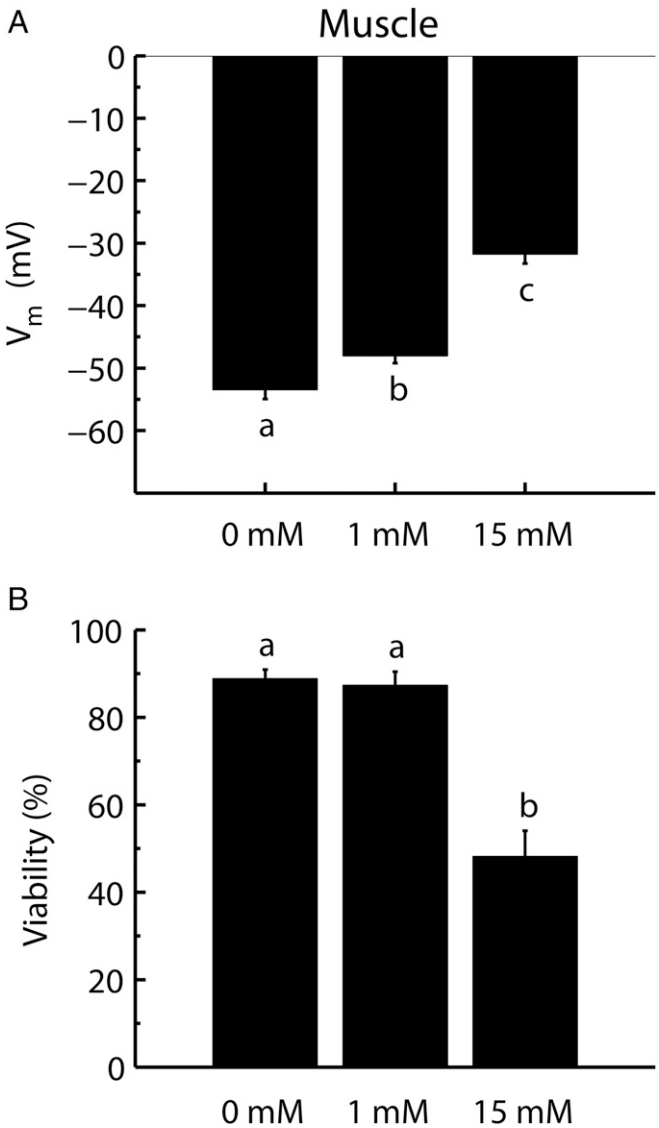

Fig. 3. Pharmacological manipulation of V_m and cellular viability using TEA. V_m (*A*) and cell viability (*B*) were measured in muscle fibers placed in a control buffer (10 mM K^+) with 0, 1, or 15 mM TEA added. Viability measurements were taken after 3 h, and V_m was measured after 5 min at 31 °C (*Materials and Methods*). Data are expressed as mean ± SEM; dissimilar letters indicate treatment groups that differ statistically (one-way ANOVA, Tukey's multiple-comparisons test, $P < 0.05$). For average V_m: $n = \geq 41$ fibers from six or more animals for each treatment; for average viabilities: $n = \geq 13$ animals for each treatment.

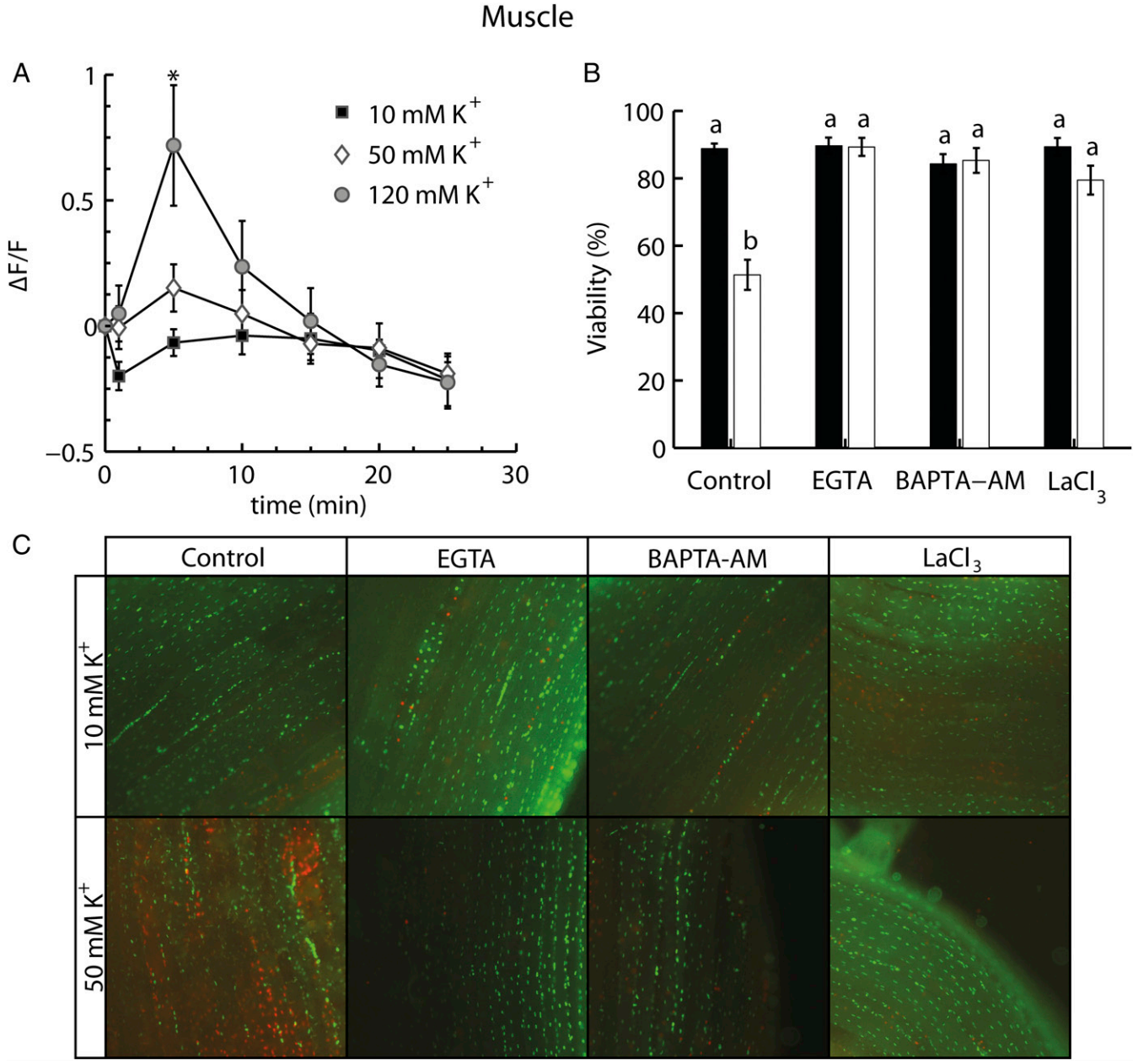

Fig. 4. The role of Ca^{2+} in depolarization-induced cell damage. (*A*) Ca^{2+} fluorescence in fibers over time exposed to 10, 50, or 120 mM K^+. (*B*) In vitro muscle fiber viability after 24 h at 0 °C using 10- or 50-mM extracellular K^+ buffers. Experiments were run in control buffer and in conjunction with the addition of EGTA (an extracellular Ca^{2+} chelator), BAPTA-AM (an intracellular Ca^{2+} chelator), or $LaCl_3$ (a Ca^{2+} channel blocker). Data are expressed as mean ± SEM; dissimilar letters indicate treatment groups that differ statistically (two-way ANOVA, Tukey's multiple-comparisons test, $P < 0.05$). The asterisk indicates a significant increase in fluorescence relative to the other groups (two-way repeated-measures ANOVA, Tukey's multiple-comparisons test, $P < 0.05$). For average viabilities: $n = \geq 9$ animals for each treatment. For average Ca^{2+} fluorescence: $n = \geq 4$ fibers from two or more animals. (*C*) Examples of composite pictures representing each treatment group (live cells are green, stained with SYBR 14, and dead cells are red, stained with PI). Each image is 750 pixels across, which corresponds to roughly 1 mm.

the addition of TEA caused cell injury in a manner that depended on the extent of depolarization (Fig. 3). Thus, cell injury developed as a consequence of depolarization regardless of whether the means of depolarization was hypothermia, hyperkalemia, or TEA and regardless of whether depolarization was elicited in muscle or ileum cells. It should be noted, however, that TEA appeared to reduce cell viability further than predicted from the depolarization alone. It is possible that this is due to other toxic effects of TEA that have been reported previously (41, 42). To compare viability experiments at different temperatures, we assumed that the processes involved in reducing viability would be affected by temperature with a Q_{10} of 2, allowing us to subject the tissues to different "chronological times" that resulted in similar "physiological exposure times" (*Materials and Methods*). Since we do not know the thermal dependence of all processes involved in cell death, it is not possible to confirm the validity of this assumption. However, we note that the standard metabolic rate of several members of *Orthoptera* has been found to scale with temperature according to Q_{10} values of 2 to 3 (43).

As mentioned previously, low temperature has been suggested to affect cell viability directly through effects on membrane fluidity and protein denaturation (18, 44). Such direct effects of low

temperature could promote K^+ leakage from the cells, suggesting that extracellular hyperkalemia develops as consequence rather than as a cause of chill injury. However, in this study, depolarization of muscles induced a similar degree of fiber injury regardless of whether the means of depolarization was temperature and/or hyperkalemia. Furthermore, in insect muscles, hypothermia has been shown to induce fiber injury without a significant loss of K^+ from the muscles even under conditions in which considerable injury has already developed (13, 23, 45). Given that hyperkalemia can induce fiber injury in a depolarization-dependent manner, hyperkalemia is clearly a mechanism of hypothermic cell injury and not merely a side effect. Thus, the results of this study support the hypothesis that chilling induces injury indirectly through depolarization in chill-susceptible insects. This strong evidence for indirect chill injury does not exclude the possibility that more severe hypothermia could also induce additional injury directly through membrane phase transitions or protein denaturation. This suggestion would be particularly interesting to examine, considering that no studies have presently investigated membrane-phase transitions directly in conjunction with chill injury in insects.

Cellular Injury Is Dependent on Ca^{2+} Availability. A prevalent theory proposes that hypothermia could induce chill injury indirectly through a depolarization-induced Ca^{2+} influx promoting apoptosis/necrosis (26, 27). To establish if hyperkalemia (depolarization) induces intracellular Ca^{2+} accumulation, we monitored cytosolic Ca^{2+} levels following injection of Fluo-4. The results show that elevated extracellular $[K^+]$ increases intracellular $[Ca^{2+}]$ in muscle fibers. This was particularly clear when fibers were subjected to 120 mM K^+, where the fluorescence signal was significantly brighter than in the other groups. Unfortunately, we also observed that the Ca^{2+} fluorescence signal decreased in all groups after 5–15 min, which restricted our ability to interpret the temporal patterns of the Ca^{2+} signal involved. The precise reason for this decrease is unknown, as Fluo-3 (a dye similar to Fluo-4) has previously been shown to be stable in other insect tissues (32). It is possible that the physiological Ca^{2+} signal involved in chill injury is only transient, but we cannot exclude the possibility that sequestration, diffusion, or enzymatic breakdown of Fluo-4 is the cause of the deteriorating signal.

We also investigated the involvement of Ca^{2+} in cold injury by exposing muscles to 24 h of 0 °C and 10 or 50 mM K^+ while manipulating both intra- and extracellular Ca^{2+} concentrations pharmacologically and subsequently measuring cell viability (Fig. 4*B*). The combination of hypothermia and hyperkalemia resulted in the development of injury only when it was possible for intracellular Ca^{2+} to accumulate. That is, the removal of the extracellular Ca^{2+} through the addition of EGTA, the removal of the intracellular Ca^{2+} through the addition of BAPTA-AM, and blocking the Ca^{2+} channels entirely prevented the injury observed in the hyperkalemic control. This clearly demonstrates that cellular injury during hypothermia/hyperkalemia is mediated by a Ca^{2+} signaling pathway. The observation that removal of extracellular Ca^{2+} alone can block the onset of injury implies that the principal source of the Ca^{2+} signaling originates from the extracellular environment rather than from the organelles. The fact that the addition of an intracellular Ca^{2+} chelator also prevents injury suggests that the extracellular Ca^{2+} must cross the membrane to induce injury. Finally, the removal of depolarization-induced injury after blocking of Ca^{2+} channels suggests that voltage-gated L-type Ca^{2+} channels are important in sensing the depolarization and thus permitting Ca^{2+} influx. It is not precisely determined how long intracellular Ca^{2+} is affected by hyperkalemia, but there is at least an initial influx of Ca^{2+} following depolarization and this influx is important to determine cell viability. Taken together, these results show that Ca^{2+} regulation is centrally involved in hypothermia-induced cell death.

Proposed Role for Ca^{2+} in Hypothermia. Determining exactly how Ca^{2+} influx causes the loss of cell viability is beyond the scope of this paper. Hypothermia has previously been shown to cause apoptosis in *Drosophila* and flesh flies (36, 37), and depolarization is a known early event of apoptosis in mammalian cells (46). Therefore our findings suggest that depolarization stimulates a cellular influx of Ca^{2+} that initiates the loss of cell viability through apoptotic or necrotic cascades (47, 48). It is interesting that hypothermia is also linked with cellular Ca^{2+} influx, cytosolic Ca^{2+} accumulation, and apoptosis in both plants and mammals (28–30, 33, 34). Thus, Ca^{2+} accumulation and apoptosis generally seem to be linked to hypothermia. Our study agrees with this view and adds that, in insect muscles and ileum tissue, depolarization seems to be the mechanistic link that initiates Ca^{2+} influx and cell damage. Particularly in insect muscles, the abundant voltage-gated L-type Ca^{2+} channel provides a plausible mechanistic link between depolarization and Ca^{2+} influx. This link is likely to be species and organ dependent. Thus, in mammalian and plant cells, hypothermic Ca^{2+} influx has been shown to be facilitated by alternative pathways rather than by voltage-sensitive Ca^{2+} channels (28–30). Hypothermia-induced Ca^{2+} influx has previously been demonstrated in insects (31, 32) and was suggested to act as a cold sensor. In these previous studies, Ca^{2+} prevented cell injury by promoting rapid cold hardening, as blocking Ca^{2+} channels reduced cell survival following hypothermia. Therefore, it seems that Ca^{2+} has a dual role in hypothermia: Low influxes of Ca^{2+} at moderate hypothermic exposure may promote cell survival by signaling rapid cold hardening, whereas higher influxes of Ca^{2+} reduce cell survival through apoptosis/necrosis. The dualistic effect of Ca^{2+} following hypothermia is also seen in plants, where Ca^{2+} accumulation is associated with the induction of cold tolerance or apoptosis depending on the circumstances (29, 30, 34). These observations conform with the widely accepted hypothesis that the downstream effect of a Ca^{2+} signal is highly dependent on the intensity/frequency of the signal (49). In the present study, a V_{m50} occurred when the membrane was depolarized to about −14 mV regardless of whether the muscles were kept at high or low temperatures. This value is similar to previous observations in locust muscles (23) in which the V_{m50} was −17 mV. Based on these observations, it is tempting to suggest the existence of a critical threshold of polarization that, once exceeded, is responsible for cell death. However, such a threshold is unlikely to be a constant across species and may depend on a large array of physiological factors, including the duration of the cold exposure. Given the involvement of Ca^{2+} channels in the promotion of hypothermic cell injury and the dependence of this injury on membrane polarization, we suggest that the value for V_{m50} could be highly dependent on the regulation of L-type Ca^{2+} channels. It is also possible that the intracellular concentration of Ca^{2+} is influenced by other mechanisms, such as the loss of active transport of Ca^{2+} across the sarcolemma or into organelles (50). Thus, temperature could be expected to affect cell injury by affecting active transport of Ca^{2+}. In any case, the present study clearly demonstrates that at the examined temperatures depolarization was a principal determinant of cell injury (Fig. 1) and strongly suggests the involvement of voltage-gated Ca^{2+} channels in chill injury. For example, we did not observe injury when cells were exposed to hypothermia (which decreases active Ca^{2+} transport) in the absence of hyperkalemia, demonstrating that reduced active transport alone was insufficient to cause Ca^{2+} overload.

In conclusion, we show that depolarization is a principal mechanism for the induction of chill injury in insects. Depolarization promotes chill injury, possibly through an apoptotic/necrotic pathway, by increasing the influx of Ca^{2+} from the extracellular side to the intracellular side. Blocking Ca^{2+} channels using $LaCl_3$ prevents chill injury, indicating that L-type Ca^{2+}

channels represent an important pathway for pathological Ca^{2+} influx. It is well known that an insect's susceptibility to accumulate chill injury varies enormously with thermal acclimation, adaptation, and the duration of the cold exposure (14, 15). These differences in chill susceptibility can often be associated with varying degrees of cold-induced hyperkalemia (and therefore depolarization), but virtually nothing is known about how acclimation or adaptation affects the electrophysiological characteristics of cells. Considering the involvement of Ca^{2+} signaling in chill injury, we propose that future studies should investigate further how acclimation and adaptation affect Ca^{2+} handling at low temperature in insects.

Materials and Methods

Experimental Animals. Animals (*Locusta migratoria*, Linnaeus 1758) used in this study were purchased from a commercial supplier (Peter Andersen ApS). Animals, with roughly a 1:1 sex ratio, arrived as fourth- to fifth-instar juveniles and were reared in well-ventilated 0.45-m^3 cages placed in a temperature-controlled room set to 25 °C. Cages were supplied with a 150-W heat lamp set to a 12-h:12-h day:night cycle and were supplied with cardboard egg cartons and steel mesh nets. This created a heterogeneous thermal environment with a roughly 25–45 °C thermal gradient which allowed the locusts to behaviorally thermoregulate during light hours. Locusts had ad libitum access to food (fresh wheat sprouts and dry wheat bran) and water and were maintained under these conditions until fully mature (sixth instar, imago). Before experiments, adult locusts (age 1–5 wk) were placed inside a cooling incubator (series KB 8000; Termaks A/S) set to 31 °C for 3–5 d to ensure that all animals were preacclimated to similar thermal conditions.

Tissue Preparation. Most experiments in this study were conducted using the mesothoracic posterior tergocoxal muscle, M90 (51). To examine if the relation between V_m and cellular viability extended to other tissue types, we also performed experiments on hindgut tissue, specifically the ileum.

Before experiments, locust heads were removed, and a ventral longitudinal incision was made across the thorax using fine scissors. The preparations were carefully pinned down (ventral side up) in Petri dishes with a silicone elastomer base (Sylgard 184; Dow Corning Corp) and were submerged in pretempered locust buffer for incubation (see below). For experiments on muscle tissue, the mesothoracic posterior tergocoxal muscle was exposed using fine-pointed forceps to carefully remove the gut and fat bodies. For experiments using ileal tissue, we used a similar protocol but removed only the fat bodies and Malpighian tubules. All dissections were carried out at room temperature under a stereomicroscope.

Experimental Setup. Using muscle and ileum preparations, we estimated in situ cellular V_m and in vitro viability following a range of chemical and pharmacological interventions that manipulated V_m and Ca^{2+} availability. These experiments were performed at either 31 °C or 0 °C. Because biological processes proceed faster at high temperatures, we assumed a Q_{10} of 2 to create a comparable physiological exposure time for experiments run at different temperatures. Thus, viability experiments at 0 °C were performed with 24 h of exposure to the experimental buffer, while similar experiments at 31 °C were assessed after 3 h of exposure. Similarly, V_m was measured after the muscle had equilibrated with the experimental buffer for 45 and 5 min at 0 °C and 31 °C, respectively. Throughout the experiments we routinely measured the temperature of the preparations and experimental setups using K-type thermocouples connected to a TC-08 data logger (Pico Technology).

Buffers and Pharmacological Agents. Buffer solutions were based on a locust buffer recipe from Hoyle (38) previously used for viability and V_m measurements (23, 24): basal conditions: 10 mM KCl, 140 mM NaCl, 3 mM $CaCl_2$, 2 mM $MgCl_2$, 1 mM NaH_2PO_4, 90 mM sucrose, 5 mM glucose, 5 mM trehalose, 1 mM proline, 10 mM Hepes, adjusted to pH 7.2 using NaOH. In experiments with hypo- and hyperkalemia, osmolality was maintained by substituting KCl for NaCl. Manipulation of V_m through pharmaceutical means was done by adding TEA in concentrations of 1 or 15 mM and subsequently measuring V_m after 15–30 min. To examine the role of Ca^{2+} regulation in the development of chill injury, we used three pharmacological agents, EGTA, BAPTA-AM, and $LaCl_3$, to manipulate the availability of extracellular Ca^{2+}, intracellular Ca^{2+}, and transmembrane Ca^{2+} flux, respectively. Thus, in experiments to exclude extracellular Ca^{2+}, we replaced $CaCl_2$ with $MgCl_2$ and added 500 μM EGTA, a membrane impermeable Ca^{2+} chelator. In experiments to remove intracellular Ca^{2+}, we used 100 μM BAPTA-AM, a membrane permeable Ca^{2+} chelator. BAPTA-AM was solubilized in DMSO before it was added to the buffer. In these experiments the muscle preparations were bathed in the BAPTA-AM solution for 60 min, after which the preparations were rinsed twice in fresh buffer with the desired K^+ concentration (without BAPTA-AM). Finally, we performed experiments with 250 μM $LaCl_3$, a blocker of Ca^{2+} channels; in these experiments NaH_2PO_4 was removed from the buffer to prevent precipitation of lanthanum phosphate.

Measurement of V_m. V_m was measured by fixing the opened animals in jacketed glass Petri dishes with the mesothoracic posterior tergocoxal muscle or ileum freely accessible and submerged in ∼10 mL of the experimental buffer. The temperature of the preparation was maintained by pumping cooling liquid through the jacketed glass Petri dish using a temperature-controlled water bath. V_m were measured using a chlorinated silver wire as a reference electrode and inserting a Clark borosilicate glass microelectrode (1B150F-4; World Precision Instruments, Inc.) into the cells. Glass electrodes were pulled using a Flaming-Brown P-97 electrode puller (Sutter Instruments Co.) and were backfilled with 3 M KCl saline to have a resistance of roughly 15–30 MΩ. An Electro 705 electrometer (World Precision Instruments, Inc.) served as the central hub to which both reference and measuring electrodes were connected. Data were digitalized using a Micro1401-3 data-acquisition system (Cambridge Electronic Design) and were recorded using Spike2 software (v8,0; Cambridge Electronic Design). Membrane penetrations were registered as sudden drops in electrical potential, which were interpreted as the electrode having successfully entered the cell. The microelectrode was then retracted and reinserted for a minimum of three stable repeats representative of that particular cell, after which the electrode was moved to locate a new cell, and the procedure was repeated. The procedure was typically repeated for 10 min or until the V_m of eight separate cells in one individual animal had been measured. For each cell, the V_m is reported as the average of the repeated recordings. All V_m reported in this study are based on measurements of at least five or six animals per treatment.

Cellular Viability. Cellular viability was quantified with a LIVE/DEAD sperm viability kit (Thermo Fisher Scientific) used successfully in previous studies to assess viability in insect tissue (23, 24, 32, 37). The LIVE/DEAD kit contains two fluorescent stains: SYBR 14 (excitation λ_{max}: 475 nm, emission λ_{max}: 516 nm) and propidium iodide (PI; excitation λ_{max}: 535 nm, emission λ_{max}: 617 nm). Both dyes have high affinity toward the nucleotide constituents of the cell, resulting in a dye–nucleus complex that emits either green (SYBR 14) or red (PI) florescent light when excited by visible light. SYBR 14 is membrane permeable and will stain all nuclei, while PI is membrane impermeable and thus only stains cells in which the membrane integrity has been compromised (52, 53). Accordingly, live cells will be stained green, and dead cells will be stained red.

To examine cellular viability, tissue preparations were fixed in a large Petri dishes, submerged in ∼50 mL experimental buffer solution, and sealed shut to prevent evaporation or condensation during the experimental exposure. Following treatment, the tissue of interest (muscle or ileum) was carefully dissected out and placed on a glass slide. For dissections of the gut, the gut was sealed at both ends with suture to prevent the high levels of K^+ present in the gut from leaking out. Subsequently, tissues were removed from the preparation and placed on a glass slide where they were submerged in 30 μL experimental buffer containing SYBR14 (40 μM). Here, tissues were incubated for 10 min; then 30 μL of experimental buffer containing PI (84 μM) was added, and the tissues were incubated for an additional 10 min, after which the samples were ready for imagining. A coverslip was gently placed on top of the preparation that was then imaged using a Zeiss Axio Imager. A2 fluorescence microscope (Carl Zeiss AG). To determine the extent of DNA staining by SYBR14 or PI, appropriate filters were used to fit with the emission characteristics of these dyes.

Cell viability was calculated by counting the number of nuclei stained by SYBR14 and PI, respectively. This was done using Fiji computer software using methods similar to those of MacMillan et al. (24). Representative pictures of stained muscle fibers are presented in Figs. 1*D* and 4*C*.

Ca^{2+} Imaging. In these experiments, femur muscle fibers were used instead of mesothoracic posterior tergocoxal muscles, as this allowed us to extract muscles with intact fibers and mount them in our measurement chamber. To access the muscle fibers, approximately two-thirds of the femur was isolated by removing the coxa, trochanter, and the distal part of the femur, and an incision was made along the dorsal and ventral side of the femur. This preparation was mounted in an experimental chamber with a Sylgard (Dow Corning) bottom by pinning needles through the exoskeleton to expose

the fibers. The retractor unguis muscle was then removed to expose fibers of the extensor tibia. The experimental chamber was placed in an upright microscope at room temperature (*ca*. 23 °C), and the fibers were immersed in basal 10-mM KCl locust buffer without $CaCl_2$. The muscle was allowed to rest for at least 5 min before one to three fibers were injected with Fluo-4 pentapotassium salt (Thermo Fisher Scientific) using sharp electrodes backfilled with the dye and connected to a TEC-05X amplifier. The dye was injected for about 4 min using a constant 20-nA current. After injection, fibers rested for at least 5 more minutes before imaging began. The dye was excited using a polychrome V monochromator system (TILL Photonics) using light with a wavelength of 488 nm, and Ca^{2+} signals were recorded using a Nikon DS-Vi1 color microscope camera (Ramcon) using an exposure time of 100 ms and a gain of 2×. The fluorescence intensity was recorded using the NIS elements D 4.1 software (Ramcon). Using this software, we measured an intensity profile over a distance of about 280 μm and roughly parallel to the fibers. After an adequate resting period postinjection, the fluorescence was measured in the Ca^{2+}-free buffer, and then the buffer was changed, as previously described, to a buffer containing 3 mM Ca^{2+} and 10/50/120 mM K^+. The fluorescence intensity was measured immediately following the buffer change and then every 5 min for 25 min. The fluorescence intensity was expressed as $\Delta F/F$ where F is the fluorescence intensity in the Ca^{2+}-free buffer and ΔF is the change in intensity from F.

Data Analysis. All statistical analyses were performed as ANOVA. When a significant difference was identified, a Tukey's multiple-comparisons test was used to separate treatment groups differing statistically ($P < 0.05$). All data are expressed as mean ± SEM.

ACKNOWLEDGMENTS. J.S.B., O.B.N., T.H.P., and J.O. were funded by Aarhus University Research Foundation (AUFF) NOVA. J.O. was funded by The Danish National Council for Independent Research Natural Sciences.

1. Gunderson AR, Stillman JH (2015) Plasticity in thermal tolerance has limited potential to buffer ectotherms from global warming. *Proc Biol Sci* 282:20150401.
2. Sunday JM, Bates AE, Dulvy NK (2010) Global analysis of thermal tolerance and latitude in ectotherms. *Proc Biol Sci* 278:1823–1830.
3. Addo-Bediako A, Chown SL, Gaston KJ (2000) Thermal tolerance, climatic variability and latitude. *Proc Biol Sci* 267:739–745.
4. Kellermann V, et al. (2012) Phylogenetic constraints in key functional traits behind species' climate niches: Patterns of desiccation and cold resistance across 95 Drosophila species. *Evolution* 66:3377–3389.
5. Chown SL, Terblanche JS (2006) Physiological diversity in insects: Ecological and evolutionary contexts. *Adv In Insect Phys* 33:50–152.
6. Ramløv H (2000) Aspects of natural cold tolerance in ectothermic animals. *Hum Reprod* 15:26–46.
7. Duman JG (2001) Antifreeze and ice nucleator proteins in terrestrial arthropods. *Annu Rev Physiol* 63:327–357.
8. Zachariassen KE (1985) Physiology of cold tolerance in insects. *Physiol Rev* 65:799–832.
9. Bale JS (1996) Insect cold hardiness: A matter of life and death. *Eur J Entomol* 93: 369–382.
10. Toxopeus J, Sinclair BJ (2018) Mechanisms underlying insect freeze tolerance. *Biol Rev Camb Philos Soc,* 10.1111/brv.12425.
11. Bale JS (1993) Classes of insect cold hardiness. *Funct Ecol* 7:751–753.
12. Sinclair BJ (1999) Insect cold tolerance: How many kinds of frozen? *Eur J Entomol* 96: 157–164.
13. Kostál V, Yanagimoto M, Bastl J (2006) Chilling-injury and disturbance of ion homeostasis in the coxal muscle of the tropical cockroach (Nauphoeta cinerea). *Comp Biochem Physiol B Biochem Mol Biol* 143:171–179.
14. Kostál V, Vambera J, Bastl J (2004) On the nature of pre-freeze mortality in insects: Water balance, ion homeostasis and energy charge in the adults of Pyrrhocoris apterus. *J Exp Biol* 207:1509–1521.
15. Overgaard J, MacMillan HA (2017) The integrative physiology of insect chill tolerance. *Annu Rev Physiol* 79:187–208.
16. MacMillan HA, Sinclair BJ (2011) The role of the gut in insect chilling injury: Cold-induced disruption of osmoregulation in the fall field cricket, Gryllus pennsylvanicus. *J Exp Biol* 214:726–734.
17. Nedvěd O, Lavy D, Verhoef HA (1998) Modelling the time-temperature relationship in cold injury and effect of high-temperature interruptions on survival in a chill-sensitive collembolan. *Funct Ecol* 12:816–824.
18. Quinn PJ (1985) A lipid-phase separation model of low-temperature damage to biological membranes. *Cryobiology* 22:128–146.
19. Arav A, et al. (1996) Phase transition temperature and chilling sensitivity of bovine oocytes. *Cryobiology* 33:589–599.
20. Hazel JR (1995) Thermal adaptation in biological membranes: Is homeoviscous adaptation the explanation? *Annu Rev Physiol* 57:19–42.
21. Zachariassen KE, Kristiansen E, Pedersen SA (2004) Inorganic ions in cold-hardiness. *Cryobiology* 48:126–133.
22. Macmillan HA, Sinclair BJ (2011) Mechanisms underlying insect chill-coma. *J Insect Physiol* 57:12–20.
23. Andersen MK, Folkersen R, MacMillan HA, Overgaard J (2017) Cold acclimation improves chill tolerance in the migratory locust through preservation of ion balance and membrane potential. *J Exp Biol* 220:487–496.
24. MacMillan HA, Baatrup E, Overgaard J (2015) Concurrent effects of cold and hyperkalaemia cause insect chilling injury. *Proc Biol Sci* 282:20151483.
25. Wareham AC, Duncan CJ, Bowler K (1974) The resting potential of cockroach muscle membrane. *Comp Biochem Physiol A* 48:765–797.
26. Hochachka PW (1986) Defense strategies against hypoxia and hypothermia. *Science* 231:234–241.
27. Boutilier RG (2001) Mechanisms of cell survival in hypoxia and hypothermia. *J Exp Biol* 204:3171–3181.
28. Haddad P, Cabrillac JC, Piche D, Musallam L, Huet PM (1999) Changes in intracellular calcium induced by acute hypothermia in parenchymal, endothelial, and Kupffer cells of the rat liver. *Cryobiology* 39:69–79.
29. Knight H, Trewavas AJ, Knight MR (1996) Cold calcium signaling in Arabidopsis involves two cellular pools and a change in calcium signature after acclimation. *Plant Cell* 8:489–503.
30. Monroy AF, Sarhan F, Dhindsa RS (1993) Cold-Induced changes in freezing tolerance, protein phosphorylation, and gene expression. *Plant Physiol* 102:1227–1235.
31. Teets NM, et al. (2008) Rapid cold-hardening in larvae of the Antarctic midge Belgica Antarctica: Cellular cold-sensing and a role for calcium. *Am J Physiol Regul Integr Comp Physiol* 294:R1938–R1946.
32. Teets NM, Yi S-X, Lee RE, Jr, Denlinger DL (2013) Calcium signaling mediates cold sensing in insect tissues. *Proc Natl Acad Sci USA* 110:9154–9159.
33. Anderson CD, et al. (2004) Mitochondrial calcium uptake regulates cold preservation-induced Bax translocation and early reperfusion apoptosis. *Am J Transplant* 4:352–362.
34. Chen J, et al. (2014) The role of ethylene and calcium in programmed cell death of cold-stored cucumber fruit. *J Food Biochem* 38:337–344.
35. Salehipour-Shirazi G, Ferguson LV, Sinclair BJ (2017) Does cold activate the Drosophila melanogaster immune system? *J Insect Physiol* 96:29–34.
36. Yi S-X, Moore CW, Lee RE, Jr (2007) Rapid cold-hardening protects Drosophila melanogaster from cold-induced apoptosis. *Apoptosis* 12:1183–1193.
37. Yi S-X, Lee RE, Jr (2011) Rapid cold-hardening blocks cold-induced apoptosis by inhibiting the activation of pro-caspases in the flesh fly Sarcophaga crassipalpis. *Apoptosis* 16:249–255.
38. Hoyle G (1953) Potassium ions and insect nerve muscle. *J Exp Biol* 30:121–135.
39. Dawson J, Djamgoz MBA, Hardie J, Irving SN (1989) Components of resting membrane electrogenesis in Lepidopteran skeletal muscle. *J Insect Physiol* 35:659–666.
40. Djamgoz MBA (1987) Insect muscle: Intracellular ion concentrations and mechanisms of resting potential generation. *J Insect Physiol* 33:287–314.
41. Elliott RC (1987) The role of acetylcholine in tetraethylammonium induced contractures of the chick biventer cervicis muscle in the presence of lidocaine. *Gen Pharmacol* 18:7–11.
42. Elliott RC (1982) The actions of tetraethylammonium at the neuromuscular junction. *Gen Pharmacol* 13:11–14.
43. Mispagel ME (1981) Relation of oxygen-consumption to size and temperature in desert arthropods. *Ecol Entomol* 6:423–431.
44. Privalov PL (1990) Cold denaturation of proteins. *Crit Rev Biochem Mol Biol* 25: 281–305.
45. MacMillan HA, Findsen A, Pedersen TH, Overgaard J (2014) Cold-induced depolarization of insect muscle: Differing roles of extracellular K+ during acute and chronic chilling. *J Exp Biol* 217:2930–2938.
46. Bortner CD, Gómez-Angelats M, Cidlowski JA (2001) Plasma membrane depolarization without repolarization is an early molecular event in anti-Fas-induced apoptosis. *J Biol Chem* 276:4304–4314.
47. Nicotera P, Orrenius S (1998) The role of calcium in apoptosis. *Cell Calcium* 23:173–180.
48. Mattson MP, Chan SL (2003) Calcium orchestrates apoptosis. *Nat Cell Biol* 5: 1041–1043.
49. Berridge MJ, Lipp P, Bootman MD (2000) The versatility and universality of calcium signalling. *Nat Rev Mol Cell Biol* 1:11–21.
50. Orrenius S, Zhivotovsky B, Nicotera P (2003) Regulation of cell death: The calcium-apoptosis link. *Nat Rev Mol Cell Biol* 4:552–565.
51. Snodgrass RE (1929) The thoracic mechanism of a grasshopper and its antecedents. *Smithson Misc Collect* 82:1–111.
52. Garner DL, Johnson LA (1995) Viability assessment of mammalian sperm using SYBR-14 and propidium iodide. *Biol Reprod* 53:276–284.
53. Garner DL, Johnson LA, Yue ST, Roth BL, Haugland RP (1994) Dual DNA staining assessment of bovine sperm viability using SYBR-14 and propidium iodide. *J Androl* 15: 620–629.